Original Article

Optimization of constrained layer damping for strain energy minimization of vibrating pads

Supachai Lakkam[1]* and Saiprasit Koetniyom[2]

[1] *Department of Mechanical Engineering*
Rajamankara University of Technology Pranakhon, Dusit, Bangkok, 10300 Thailand.

[2]*The Sirindhorn International Thai-German Graduate School of Engineering*
King Mongkut's University of Technology North Bangkok, Bang Sue, Bangkok, 10800 Thailand.

Abstract

An optimization study for brake squeals aims to minimize the strain energy of vibrating pads with constrained layer damping. To achieve this, using finite element method and experiments were operated and assumed-coupling mode method was used to solve it. The integrated global strain energy of the pad over a frequency range of interesting mode was calculated. Parametric studies were then performed to identify those dominant parameters on the vibration response of the damped pad. Moreover, the proposed methodology was employed to search for the optimum of the position/geometry of the constrained layer damping patch. Optimal solutions are given and discussed for different cases where the strain energy of the pad over a frequency range is covering the first bending mode and with the inclusion of the restriction of minimum damping material utilization. As a result, the integrated strain energy is then performed to identify and optimize the position and geometry of the damping shim. The optimization of the constrained layer damping for strain energy minimization of vibrating pads depend on the position of the shape of the damping patch. These data can guide to specify the position of the constrained layer damping patch under pressure conditions.

Keywords: disc brake noise, friction coefficient, damping shim

1. Introduction

It is principally accepted that noise and vibration have become key issues in the intention of automotive braking systems. Typically, the vibration of a brake system cause brake noise phenomena. There are several methods to reduce brake noise phenomena. One of the brake noise reduction methods is the addition of a constrained layer material to the brake pads (Triches *et al.*, 2004 and Zheng *et al.*, 2004). For the control strategy of vibration, there are many parameters to indicate the degree of vibration. Displacement/acceleration of deformation, loss factor/damping ratio, vibration energy and strain energy are examples for controlling strategies. In mechanical engineering aspects, the global strain energy is simply used as an indicator for vibration of the brake system in order to optimize the constrained layer damping.

2. Literature survey

2.1 Experimental works

Generally, the experimental works focus on how to reduce brake noise behavior which can be classified based on the approaching procedure. The first approach is the active or direct method that is used to prevent the source of sound vibration in the brake system. Secondly, it is called passive or indirect method, which is mainly to minimize the sound

---

* Corresponding author.
  Email address: bus_supachai@hotmail.com

vibration.

In direct methods, the characteristic of disc brake squeal was investigated (Eriksson *et al.*, 2000). The onset and suppression of such vibration have been controlled using a surface improvement of the brake disc with a grit-blasted sector. In this way, the whole pads can slide through the untreated and treated disc surface alternatively. Normally the untreated surface can generate squeal while the pad is passing. In the other method, the treated or grit-blasted surface can deactivate the vibration in the vertical plane of the brake disc. Thus, brake squeal can be eliminated with an improvement of the disc surface. However, the squeal can occur if the treated surface is wear out under long term usage.

Additionally, the basic mechanism of instability of the disc brake system was presented by Fieldhouse (2000). The propensity of brake noise generation is investigated over a range of temperatures and pressures under specific conditions through the brake disc configuration. A mechanically induced offset centre of pressure between the pad and rotor can be varied in order to investigate disc brake squeal. Consequently, the offset centre of pressure can be used to diminish disc brake squeal.

Likewise, brake squeal was reduced by the design of the friction interface between the piston and the damping shim with holes (Heppes, 2000). In this interface, the geometry of the insulator is modified to shift the center of pressure. However, the brake disc geometry is also sensitive to the center of pressure at the friction interface. With an adequate interface design, it is possible to minimize the brake squeal. Nevertheless, as both techniques are using modified interface and surface treatment they are complicated and costly during the manufacturing process.

2.2 Analytical and numerical methods

The friction material model which is able to describe the onset of self-excited vibrations from a dry friction material was suggested by Shin *et al.* (2002). The model, based on this assumption, can produce self-excited vibrations in the case of a one–degree of freedom. Consequently, only horizontal vibration of variously planar material model plays a dominant role in the case of brake squeal. Furthermore, the damping material and friction force are the key for vibration behavior. However, the model was created in one direction, which does not describe the other degrees of freedom, i.e. vertical direction. Nevertheless, the technique is typical for describing self-excited vibrations based on a dry friction model.

Additionally, the friction-induced vibration of an elastic slider was studied using a rotating disc (Ouyang *et al.*, 1999). All models were created with an elastic material behavior in both vertical and horizontal direction. However, the slider model against the disc model has flexibility and damping in the circumferential (in-plane) and transverse directions. In the boundary conditions, the static and dynamic friction coefficients were taken into this analysis. In addition, two

coupled equations of the motion between the slider and the disc models were used to obtain vibration characteristics.

A specialized mathematical modeling technique was applied for high frequency disc brake squeal analysis (Flint, 2000). This technique is used for modeling two rigid caliper parts, two lumped mass piston, two flexible pads, and disc. The complex vibration behavior of continuous elements in the model system with limited number of degrees of freedom is represented. Therefore, the damping between piston and caliper can be investigated. However, the results do not represent the responses from the disc model in circumferential direction.

Apart from the analytical model, the disc brake squeal was investigated using the finite element (FE) software named ABAQUS version 6.4 (Liu *et al.*, 2007). This method uses nonlinear static analysis to calculate the friction coupling based on the complex Eigenvalue method. Therefore, the effects of system parameters can be investigated, such as the hydraulic pressure, the rotational velocity of the disc, the friction coefficient of the contact interactions between the pads and the disc, and the stiffness of the disc and the back plates.

Moreover, the geometric nonlinear solution was studied using MSC/NASTRAN software for friction stiffness matrix to model the contact between the pad and rotor (Nack, 1999). This technique also introduces frictional dependent pressure of brake system but the method is insensitive to the variable pressure and velocity. Consequently, this simulation performed a guideline to reduce the squeal noise of the brake disc system

On the other hand, the influence of the tribological properties of the friction material on the vibration levels in a brake disc was investigated using a mathematical model (El-Butch, 2000). Two friction models with the variation of the friction coefficient from applied load, temperature, and velocity are modeled. As a result, the effect of pressure, temperature and sliding velocity on the friction coefficient depends on the choice of the friction material. For this reason, this method can be used to avoid vibration for friction. It can also be used during the early stage of design in order to minimize brake noise characteristics.

3. Characterization of the Dynamics of Brake Components

Brake noise occurs only when components of the brake system demonstrate resonance vibrations. Therefore, it is very important to determine the modal behavior of the components to understand the problem. In the following different analyses to obtain vibration behavior of a brake system are presented.

3.1 Modal simulation of brake disc

The modal analysis of the rotor is likely the most important process to find and understand solutions for the disc brake noise problem. The 3D rotor model, using a tetra-
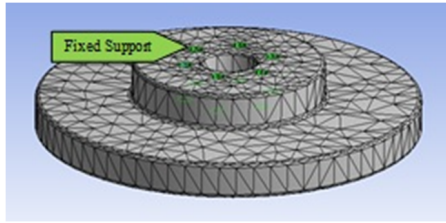
Figure 1. Fixed-free boundary conditions of brake disc

hedron element type, which consists of 20,061 nodes and 12,683 elements, is created and assumed to be constrained with bolts at the brake knuckle in order to simulate a fixed-free boundary condition as shown in Figure 1. The condition for free vibration allows the structure to vibrate without interference from other parts, making the visualization easier to locate mode shapes associated with each natural frequency. For the simulation data of the brake disc, OEM material properties of the overall brake system from Toyota PPV are used, such as the elastic modulus of 220 GPa, a Poisson's ratio of 0.3, and a density of 8,000 kg/m^3.

The simulation results of brake disc as shown in Table 1 represent its natural frequencies and degree of mode shape. Such mode shape characteristic can be seen in different frequencies between 2 and 23 kHz, which is in the range of squeal brake frequency. It also found that the degree of bending mode is proportional to the degree of response frequency. Contours of the mode shape and its frequency response for the rotor in bending modes are shown in Figure 2.

3.2 Modal analysis of brake pads

In the same way as that for the rotor model, the modal analysis of the brake pad was simulated. The 3D brake pad model using a tetrahedron element type, which consisted of 4,861 nodes and 2,541 elements, is created and supported by two slender cables in order to simulate a free-free boundary condition as shown in Figure 3. For the simulation data of the brake pad, the *Compact International*'s material properties for a Toyota PPV are used, such as the elastic modulus of 3 GPa, a Poisson's ratio of 0.23 and a density of 2,750 kg/m^3.

The mode shapes for the brake pad are very similar to the bending modes of the beams. As a consequence, the

bending modes along the longer edge occur first. From the modal coupling point of view, the bending modes are more important than the twisting modes. In most cases, the modal coupling occurs between pad and rotor bending modes. The bending mode shapes for the brake pads are shown in Figure 4 and Table 2 presents their natural frequencies. In comparison to the response frequency of the rotor, maximum response frequency of pad is less.

3.3 Analysis for coupled mode between rotor and pad

Squeal noise usually occurs whenever the interaction between pad and disc starts to vibrate together, creating a coupled system mode (Triches *et al.*, 2004). Considering the bending modes coupling, when the components have the same wavelength and frequency, they will be geometrically matched and will vibrate in the same phase. In this case, the damping characteristic of the pad is minimal. Consequently,
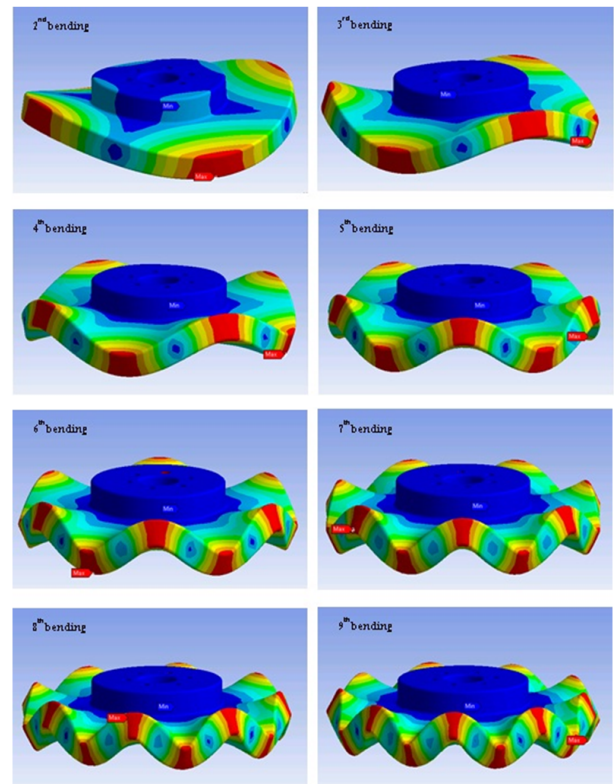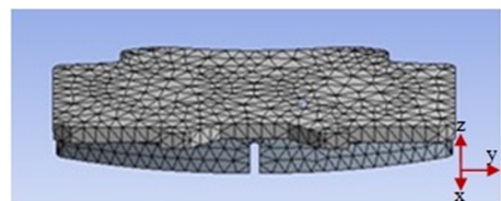

Figure 2. Various mode shapes for the rotor

Table 1. Model parameter obtained for brake disc

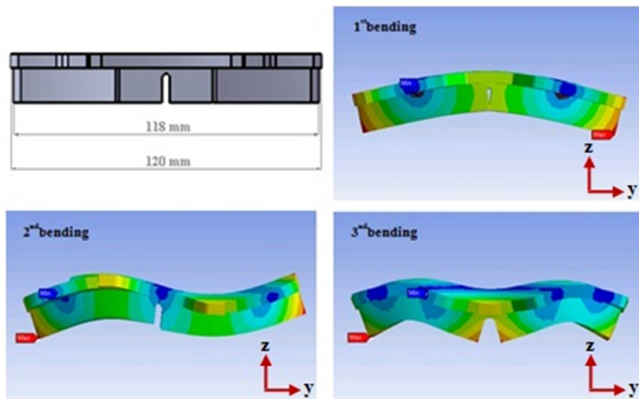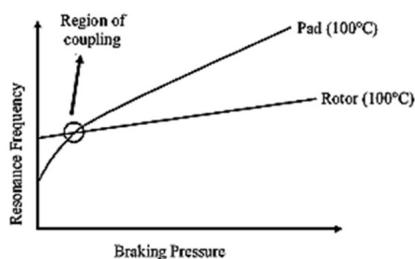| Mode Shape	Resonance Frequency(Hz)
2ndbending	2,542
3rdbending	4,433
4thbending	6,879
5thbending	9,796
6thbending	13,049
7thbending	16,532
8thbending	20,177
9thbending	23,942

Figure 3. Free-free boundary conditions of the brake pad.

Figure 4. Mode shape for brake pad

Table 2. Model parameter obtained for brake pad

Mode Shape	Resonance Frequency(Hz)
1stbending	1790
2ndbending	4953
3rdbending	8828

the brake system works as a loudspeaker, which can generate a sound pressure during coupling mode between pad and rotor. Therefore, the mode shape of the 3D rotor model is compared with the model shape of the 3D pad model in order to identify the coupling conditions. Classically, the resonance frequencies of both rotor and brake pad are significantly difference. The relation of the two modes between rotor and pad occurs when the brake system works under pressure and temperature. In this situation, the stiffness of the pad is increased moving the resonance to higher frequencies as shown in Figure 5.

To analyze for coupled modes between rotor and pad model with their geometry, it can be noticed that the first bending mode of the brake pad and the sixth bending mode of the rotor can be coupled. This coupling mode is based on the same wave length at 120 and 138 mm in both pad and rotor, respectively (see Figure 6). Thus, there is a wavelength coincidence between pad and disc in this situation, leading to

the possibility of a coupled mode in the brake system. The first bending mode of the pad has a resonance frequency around 1,790 Hz, while the rotor resonance occurs at 13,049 Hz for the sixth bending mode.

3.4 Analysis for coupled mode under pressure condition during brake application

In previous analysis, the bending modes of pad and rotor are possible to vibrate together under pressure condition. Therefore, in a simulation the pad model should be excited under pressure and constrained on the friction surface area. In this case, it is possible for the rotor to vibrate and transfer the vibration to the pad. At higher pressure conditions, the rotor and pad modes start vibrating in the same phase. In this situation, nodes of elements in both pad and rotor models are assumed not to be rotated during analysis. But they remained in the same position along the rotor diameter. For this reason, the boundary and load conditions are shown as Figure 7 in which pad surface is constrained and the back plate is applied with a pressure of 1 MPa under 30°C reference temperature. As a consequence, the friction mechanism was not taken into account. Thus, the input energy introduced by the friction between pad and rotor is replaced by the excitation from frequency response of the brake system.

3.5 Analysis for coupled mode with the damping patch under pressure condition during brake application

The simplest pad model covered with a damping patch is schematically shown in Figure 8. The model includes the back pad and the damping patch which consists of the constraining layer and the viscoelastic layer. Both constraining layer and viscoelastic core layer have the same width as the back pad. The contact model between the back pad and
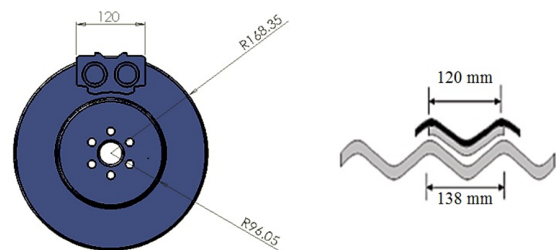

Figure 6. Wave length coincidence between disc and pad

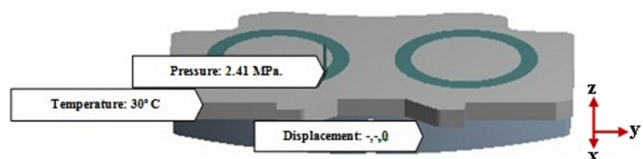Figure 5. Influence of pressure on modes of pad and disc (Triches *et al.*, 2004).

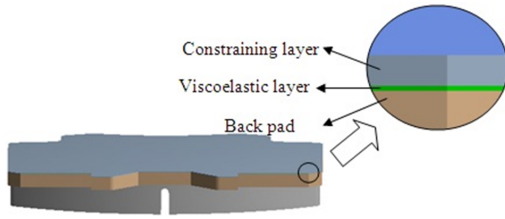Figure 7. Conditions of simulation under pressure

Figure 8. Constrained layer damping

viscoelastic layer should be unilateral. Thus, normal pressure equals zero if nodes of contact between the back pad and viscoelastic layer model is separated. In addition, gaps between them are load-dependent. Consequently, this analysis has a nonlinear load condition and the area of contact also depends on the applying load. The integrated global strain energy of the pad can also be investigated from its deformed shape of model.

4. Conceptual study

4.1 Strain energy

For the rectangular coordinate system, evaluating the work done by stresses in x direction σ_x on either side of the element, it noted that each stress acts through a different displacement. The net work done on the element by forcing all of stresses in the rectangular coordinate system ($dx\ dy\ dz$) is

$$dU = \int_0^{\varepsilon_x} \sigma_x d\varepsilon_x \left(dxdydz\right) \tag{1}$$

In the case in which σ_x, σ_y and σ_z act simultaneously, the total work done by these normal stresses is simple. Thus, the total strain energy per volume is

$$u = \frac{1}{2}\left(\sigma_x \varepsilon_x + \sigma_y \varepsilon_y + \sigma_z \varepsilon_z\right) \tag{2}$$

Because the work done by shear stress, τ_{xy} accompanying perpendicular strains γ_{yz} and γ_{xz} is zero, the total strain energy density attributable to shear alone is found by superposition of three terms identical in form with Equation 2:

$$u = \frac{1}{2}\left(\tau_{xy}\gamma_{xy} + \tau_{yz}\gamma_{yz} + \tau_{xz}\gamma_{xz}\right) \tag{3}$$

As mentioned in a general state of stress, the strain energy density is found by adding Equation 2 and 3 (Ugural et al., 1995)

$$u = \frac{1}{2}\left(\sigma_x \varepsilon_x + \sigma_y \varepsilon_y + \sigma_z \varepsilon_z + \tau_{xy}\gamma_{xy} + \tau_{yz}\gamma_{yz} + \tau_{xz}\gamma_{xz}\right) \tag{4}$$

4.2 Influence of strain energy to damping ratio for the brake pad system

To achieve optimization of the constrained layer damp-

ing patch position, only strain energy from simulation can be used in order to investigate vibration behavior for the brake pad system. This is because damping cannot be obtained from the computational results. But, it can be taken from the modal testing. Therefore, correlation between strain energy from simulation and damping ratio from experiment should be investigated in order to optimize vibration of the brake pad from strain energy using only simulation.

To find out the damping ratio of brake pad with damping patch, the vibration of the constrained layer damping patch position is performed by using a vibration test. Four different types of geometry with the constrained layer damping patch position such as no damping patch, full damping patch, two-side damping patch and three-part damping patch are illustrated in Table 3.

From testing, the experimental result reveals that these resonances from the first bending mode are slightly the same around 2.2 kHz with a damping ratio ranging from 0.0054 to 0.0189, respectively as shown in Table 4. For the simulation result using FEM, there are 1.20×10^4 to 4.29×10^4 nodes and 5.79×10^3 to 1.85×10^3 elements using a tetrahedron element type and the four different types of pad geometry are modeled as shown in Table 5.

As a result of the simulation, it reveals that the bending mode is dominated by shear strain from viscoelastic materials. The comparison of the shear strain density (in the y-z and x-z planes) of the viscoelastic layer from different positions of the constrained layer damping patch is shown in Figure 9. These results are related to the global strain energy of the pad system (see Figure 10). Nevertheless, strain energy density per damping area indicates that three-part geometry can reduce strain energy more than the two-side geometry as shown in Figure 11. This is because the shear strain energy at the middle area is more than that of other areas with a less amount of vibration.

Table 3. Position of the constrained layer damping patch for modal testing
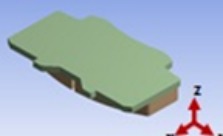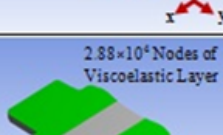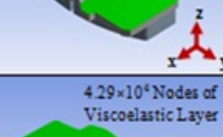
Constrained Layer Damping Patch		Damping Area(cm²)
	No Damping Patch	-
	Full Geometry (Full)	72.6
	Two-side Geometry (2 sides)	55.8
	Three-part Geometry (3 parts)	72.0

Table 4. Experimental results of the constrained layer damping patch
for vibration testing

No.	Constrained Layer Damping Patch	Natural Frequency, f_n (Hz)	Damping Ratio, D
1	No Damping Patch	2,264	0.0054
2	Full Geometry	2,258	0.0189
3	Two-side Geometry	2,233	0.0055
4	Three-part Geometry	2,233	0.0109

Table 5. Position of the constrained layer damping patch for simulation

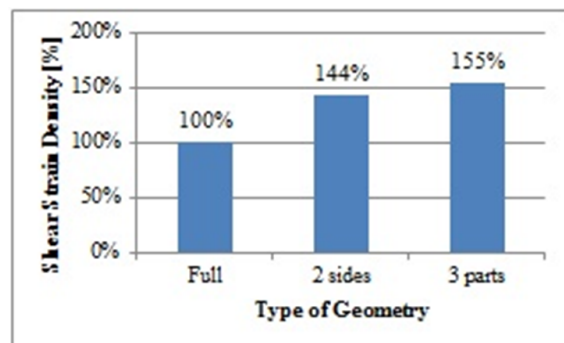| Constrained Layer Damping Patch	Damping Area(cm²)
No Damping Patch	-
Full Geometry (Full)	72.6
Two-side Geometry (2 sides)	55.8
Three-part Geometry (3 parts)	72.0

Figure 9. Simulation results for shear elastic strain of viscoelastic layer (in y-z and x-z planes)
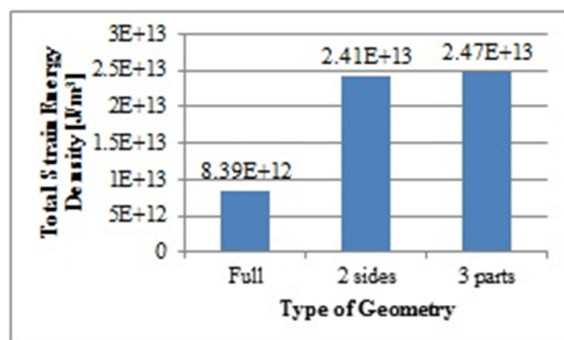

Figure 10. Simulation results for integrated global strain energy density of the viscoelastic layer
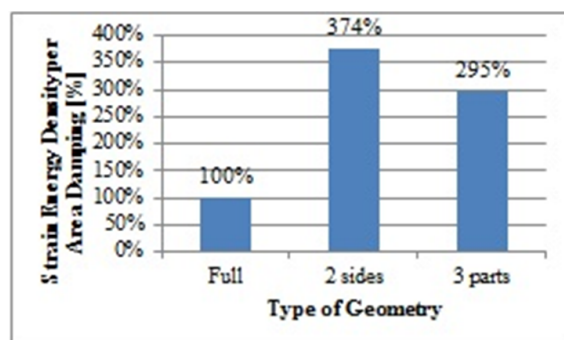

Figure 11. Simulation results for strain energy density per damping area (calculated by global strain energy divided by area) of the viscoelastic layer

From the experimental results in Table 4 and simulation results in Figure 9, 10, and 11 it can be concluded that damping ratios are in-proportional to the strain energy of the viscoelastic layer. Thus, these techniques can be used as basic knowledge for the optimization of the constrained layer damping patch in the next step in order to minimize strain energy for vibration and noise of the brake system.

5. Investigation of vibration properties and geometry for constrained layer damping

In the following, vibration properties and parameters of the geometry from the simple pad model under viscoelas-

tically damped systems are desirable to carry out parametric investigations, which dominate on the vibration response of the pad structure. The strain energy density equation of the simple pad model, Equation 4, is calculated from deformation results. The basis simulation results, the deformation of the pad are investigated. OEM material properties of the overall brake system from a Toyota PPV are used for the simulations as shown in Table 6.

5.1 Variation in the elastic modulus of the viscoelastic system

The integrated global strain energies of the pad from the variation in the elastic moduli, E_v, of the viscoelastic system between 0.3, 1.3, 2.3 and 3.3 MPa are displayed in Figure 12. In this parametric study, the thicknesses of both constraining layer and damping layer are kept constant at h_v = 0.03 mm and h_c = 0.3 mm, respectively. It can be demonstrated that viscoelastic elastic modulus plays a much more crucial role, not only in the strain energy density, but also in the resonant frequency of the brake pad system. A lower elastic modulus tends to reduce the resonant frequency and the optimization of viscoelastic strain energy is 2.3 of the viscoelastic elastic modulus. However, this is due to the fact that pad manufacturers are unable to produce lower elastic moduli of the pad. It is then estimated from the results that

there is an optimal value of the elastic modulus for the viscoelastic layer to maintain a minimization strain energy density on the pad system.

5.2 Variation of viscoelastic layer thickness

The comparison of the integrated global strain energy density of the pad using different thicknesses for the viscoelastic layer is given in Figure 13. It can be seen that lower strain energy density can be achieved in a system by increasing the thickness of viscoelastic layer. However, it is also evident that this decrease in strain energy density is not a linear function of thickness. If the viscoelastic layer thickness is too high the strain energy density can be raised. For the variation of the viscoelastic thickness no significant change of the resonant frequency of the pad is expected. It is then estimated that an optimal value of the viscoelastic layer thickness exists for a minimial strain energy density on pad system.

5.3 Variation of the constrained layer damping patch position

The position of the constrained layer damping patch is divided into six patterns based on the propensity of the strain energy, such as no damping patch, full damping patch,

Table 6. OEM part specifications

| Part name	Rotor	Friction material	Back plate	Viscoelastic layer	Constraining layer
Mechanical Properties					
Elastic modulus(Pa)	220×10^9	3×10^9	210×10^9	1.361×10^6	200×10^9
Poisson's ratio	0.3	0.23	0.3	0.39	0.3
Density(kg/m³)	8000	2750	7800	1000	7000
Thermal properties					
Thermal expansion(/K)	1.2×10^{-5}	-	1.2×10^{-5}	-	1.17×10^{-5}
Thermal conductivity(W/mK)	45	2.06	52	0.189	51.9
Specific heat (J/kgK)	510	749	486	1535	486
Geometry					
Thickness(mm)	12	9	6	0.03	0.3
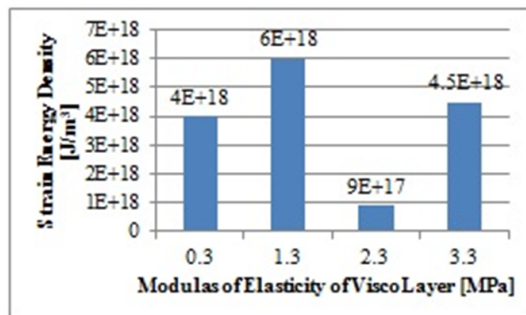
Figure 12. Integrated global strain energy density of the viscoelastic layer with various the viscoelastic's elastic modulus
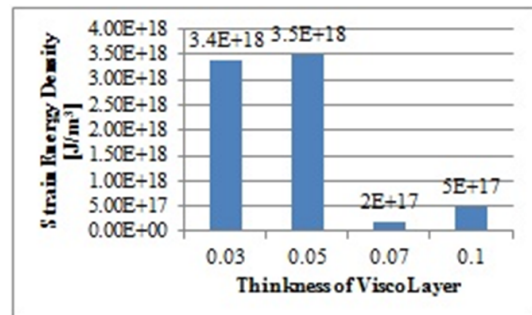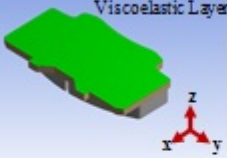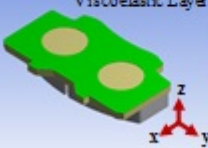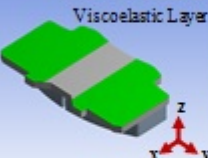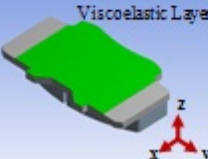

Figure 13. Integrated global strain energy density of the viscoelastic layer with a variation of the viscoelastic layer thickness

hole damping patch, finned damping patch, two-side damping patch, and a middle geometry, which are 1.20×10^4 to 5.90×10^4 nodes and 5.79×10^3 to 29.12×10^3 elements, using a tetrahedron element type as shown in Table 7.

A comparison of the shear strain densities (in y-z plane, x-z plane) of the viscoelastic layer from different positions of the constrained layer damping patch under pressure conditions is show in Figure 14. These results are related to the global strain energy under pressure conditions of the pad system (see Figure 15). Nevertheless, Figure 16 shows the same area for different patterns of the hole, two-side and middle geometry. It can be seen that the smallest strain energy density can be achieved by a full geometry of the constrained layer damping patch in the system. Furthermore, a comparison between patterns with an equal area damping reveals that the middle geometry provides the lowest strain energy density or high area efficiency that induces mode shape in the pad. This is because the cutoff area at the hole in the pad is pressed by the piston which has a small amount of vibration.

Since the strain energy density of the viscoelastic layer can be calculated through the integration for constituting the deformation shape, the broadband displacement of the pad is related to the physical and geometrical parameters of the pad itself and the viscoelastic and constraining layers. Parametric studies are preformed to recognize the important parameters of the constrained layer damping, which affect significantly the strain energy density of the damped pad. The results show that the strain energy density of the viscoelas-
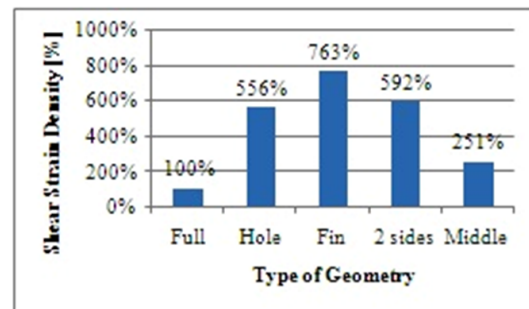

Figure 14. Shear elastic strain of the viscoelastic layer (in y-z and x-z planes) with various positions of the constrained layer damping patch

Table 7. Various position of the constrained layer damping patch

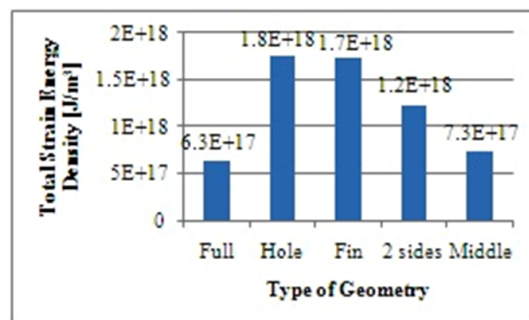| Constrained Layer Damping Patch		Damping Area(cm²)
1.20×10^4 Nodes of Viscoelastic Layer	Full Geometry (Full)	72.6
4.22×10^4 Nodes of Viscoelastic Layer	Hole Geometry (Hole)	55.8
5.90×10^4 Nodes of Viscoelastic Layer	Fin Geometry (Fin)	58.8
2.88×10^4 Nodes of Viscoelastic Layer	Two-side Geometry (2 sides)	55.8
1.98×10^4 Nodes of Viscoelastic Layer	Middle Geometry (Middle)	55.8

Figure 15. Integrated global strain energy density of viscoelastic layer with various positions of the constrained layer damping patch
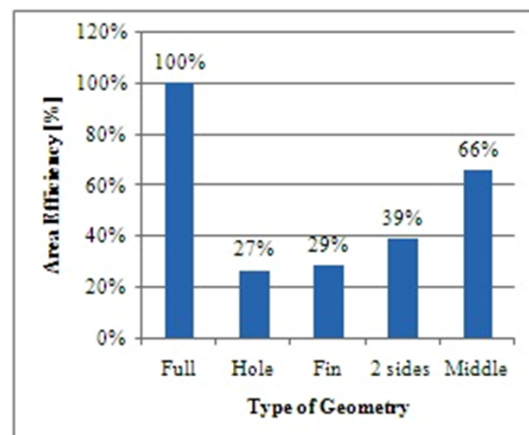

Figure 16. Area efficiency (calculated by strain energy divided by area) of the constrained layer damping patch position

tically damped pad is sensitive to the position/geometry of the constrained layer damping patch and the viscoelastic elastic modulus more than to other parameters. Thus, these techniques can be used as a basic knowledge for the optimization of the constrained layer damping treatment for strain energy minimization of vibration and noise of the brake system.

6. Conclusion

This research reveals the overall results of the experimental work and simulation. For experimental analysis from modal testing, it can be found that the influence of the strain energy to the damping ratio of a brake pad system is represented in a brake noise reduction method. According to the simulation results, the strain energy density of the viscoelastically damped pad is sensitive to the position/geometry of the constrained layer damping patch and the viscoelastic elastic modulus more than to other parameters. The optimization of the constrained layer damping for strain energy minimization of vibrating pads depends on the position of the shape of the damping patch. These data can guide to specify the position of the constrained layer damping patch under pressure conditions.

Acknowledgments

References

El-Butch, A.M.A. 2000. Evaluation of friction materials' tribological properties and their effect on the dynamic response of disc-brake systems. Proceedings of the International Conference on Brakes 2000 Automotive Braking-Technologies for the 21th Century, Leeds, UK, July 11-12, 2000, 51-60.

Eriksson, M., Bergman, P. and Jacobson, S. 2000. A study of inhibition of disc-brake squeal. Proceedings of the International Conference on Brakes 2000 Automotive Braking-Technologies for the 21th Century, Leeds, UK, July 11-12, 2000, 29-37.

Fieldhouse, J.D. 2000. A study of the interface pressure distribution between pad and rotor, the co-efficient of friction and caliper mounting geometry with regard to brake noise. Proceedings of the International Conference on Brakes 2000 Automotive Braking-Technologies for the 21th Century, Leeds, UK, July 11-12, 2000, 3-18.

Flint, J. 2000. Modeling of high frequency disc-brake squeal. Proceedings of The International Conference on Brakes 2000 Automotive Braking-Technologies for the 21th Century, Leeds, UK, July 11-12, 2000, 39-50.

Heppes, P. 2000. Brake squeal reduction by the design of the interface caliper-friction pads-brake shoe holder. Proceedings of The International Conference on Brakes 2000 Automotive Braking-Technologies for the 21th Century, Leeds, UK, July 11-12, 2000, 29-38.

Liu, P., Zheng, H., Cai, C., Wang, Y.Y., Lu, C., Ang, K.H. and Liu, G.R. 2007. Analysis of disc brake squeal using the complex eigenvalue method. Applied Acoustics. 68, 603–615.

Nack, W.V. 1999. Brake squeal analysis by finite elements and comparisons to dyno results. Proceedings of the 1999 American Society of Mechanical Engineers (ASME) Design Engineering Technical Conference, Las Vegas, Nevada, U.S.A., Sep. 12-15, 1999, DETC99/DFM-8923.

Ouyang, H., Mottershead, J.E., Cartmell, M.P. and Brookfield, D.J. 1999. Friction-induced vibration of an elastic slider on a vibrating disc. International Journal of Mechanical Sciences. 41, 325-336.

Shin, K., Brennan, M.J., Oh, J.-E. and Harris, C.J. 2002. Analysis of disk brake noise using a two-degree-of-freedom model. Journal of Sound and Vibration. 254, 837–848.

Triches, M., Gerges, N.Y. and Jordan, R. 2004. Reduction of squeal noise from disc brake systems using constrained layer damping. Journal of the Brazilian Society of Mechanical Sciences and Engineering. 26, 476-498.

Ugural, A.C. and Fenster, S.K. 1995. Advanced Strength and Applied Elasticity, Prentice-Hall PTR, New York, U.S.A., pp. 77-79.

Zhen, H., Cai, C. and Tan, X.M. 2004. Optimization of partial constrained layer damping treatment for vibrational energy minimization of vibrating beams. Computers and Structures. 82, 2493-2507.